Hybrid high-order (HHO) method for modeling and numerical simulation of seismic-acoustic wave propagation

Author : Romain Mottier[§†‡] (PhD student) **Supervision** : Alexandre Ern[†‡], Laurent Guillot[§]

[†] École nationale des ponts et chaussées (ENPC - CERMICS: `https://cermics-lab.enpc.fr/`)

[§] Commissariat à l'énergie atomique et aux énergies alternatives (CEA: `https://www.cea.fr/english`)

[‡] Institut national de recherche en sciences et technologies du numérique (INRIA - SERENA: `https://team.inria.fr/serena/`)

Context and issues - Coupling of the acoustic and elastic wave equations

Objectives

- Accurate modelisation and simulation of seismo-acoustic waves **through heterogeneous domains with complex geometries**
- Treatment of realistic cases of interest
  - ▸ **High Performance Computing (HPC)**

Issues

- Difficulty to mesh complex geometries
- High-order precision needed to accurately capture waves
  - ▸ **Hybrid discontinuous methods (HDG/HHO)**

- **Acoustic wave equation:**

$$\begin{cases} \rho_{\mathrm{F}} \partial_t \boldsymbol{v}^{\mathrm{F}}(t) + \nabla p(t) = \mathbf{0} \\ \dfrac{1}{\kappa} \partial_t p(t) + \nabla \cdot \boldsymbol{v}^{\mathrm{F}}(t) = g(t) \end{cases}$$

- **Elastic wave equation:**

$$\begin{cases} \partial_t \boldsymbol{\varepsilon}(t) - \nabla^s \boldsymbol{v}^{\mathrm{S}}(t) = \mathbf{0} \\ \rho_{\mathrm{S}} \partial_t \boldsymbol{v}^{\mathrm{S}}(t) - \nabla \cdot (\boldsymbol{\mathcal{C}} : \boldsymbol{\varepsilon}(t)) = \boldsymbol{f}(t) \end{cases}$$

- **Coupling condition:**

$$\begin{cases} [\![\boldsymbol{v}(t) \cdot \boldsymbol{n}_\Gamma]\!]_\Gamma = 0 \\ (\boldsymbol{\mathcal{C}} : \boldsymbol{\varepsilon}(t)) \cdot \boldsymbol{n}_\Gamma = p(t) \boldsymbol{n}_\Gamma \end{cases}$$

Application of HHO method to seismo-acoustic coupling

- **Approximation spaces:**
  - ▸ **Acoustic domain:** $\boldsymbol{V}^k_{\mathcal{T}_{\mathrm{F}}} := \bigtimes_{T \in \mathcal{T}_h^{\mathrm{F}}} \mathbb{P}^k\left(T; \mathbb{R}^d\right)$, $\quad \hat{V}_h^{\mathrm{F}} := \bigtimes_{T \in \mathcal{T}_h^{F}} \mathbb{P}^{k'}(T; \mathbb{R}) \times \bigtimes_{F \in \mathcal{F}_h^{\mathrm{F}}} \mathbb{P}^k(F; \mathbb{R})$
  - ▸ **Elastic domain:** $\boldsymbol{\mathcal{Z}}^k_{\mathcal{T}_{\mathrm{S}}} := \bigtimes_{T \in \mathcal{T}_h^{\mathrm{S}}} \mathbb{P}^k\left(T; \mathbb{R}^{d \times d}_{\mathrm{sym}}\right)$, $\quad \hat{\boldsymbol{V}}_h^{\mathrm{S}} := \bigtimes_{T \in \mathcal{T}_h^{\mathrm{S}}} \mathbb{P}^{k'}\left(T; \mathbb{R}^d\right) \times \bigtimes_{F \in \mathcal{F}_h^{\mathrm{S}}} \mathbb{P}^k\left(F; \mathbb{R}^d\right)$

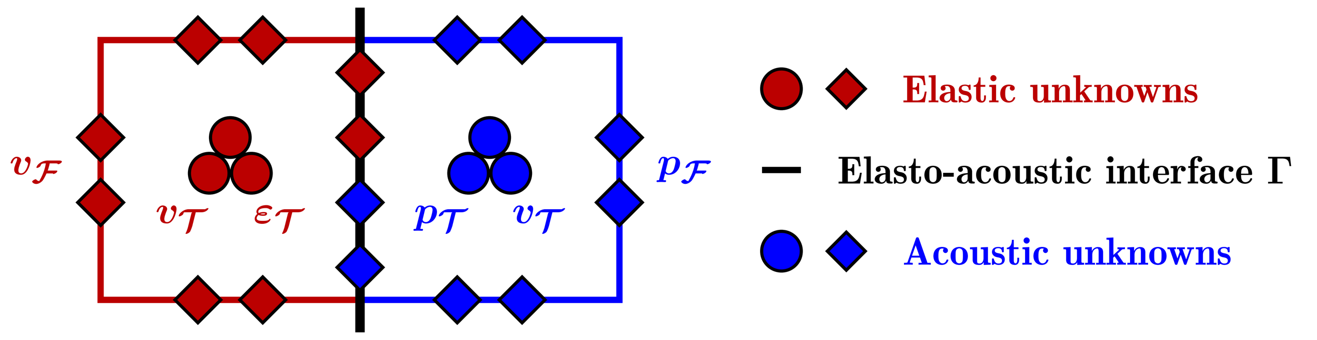

Fig. 1: Elasto-acoustic unknowns with a mixed-order ($k' = k + 1 = 2$) discretization.

- **Algebraic realization:**

$$\begin{bmatrix} \mathrm{M}^{\mathrm{v}}_{\mathcal{T}\mathcal{T}} & 0 & 0 & 0 & 0 & 0 \\ 0 & \mathrm{M}^{\mathrm{F}}_{\mathcal{T}\mathcal{T}} & 0 & 0 & 0 & 0 \\ 0 & 0 & 0 & 0 & 0 & 0 \\ 0 & 0 & 0 & \mathrm{M}^{\varepsilon}_{\mathcal{T}\mathcal{T}} & 0 & 0 \\ 0 & 0 & 0 & 0 & \mathrm{M}^{\mathrm{S}}_{\mathcal{T}\mathcal{T}} & 0 \\ 0 & 0 & 0 & 0 & 0 & 0 \end{bmatrix} \begin{bmatrix} \partial_t \mathrm{V}^{\mathrm{F}}_{\mathcal{T}} \\ \partial_t \mathrm{P}_{\mathcal{T}} \\ \partial_t \mathrm{P}_{\mathcal{F}} \\ \partial_t \mathrm{S}_{\mathcal{T}} \\ \partial_t \mathrm{V}_{\mathcal{T}} \\ \partial_t \mathrm{V}_{\mathcal{F}} \end{bmatrix} + \begin{bmatrix} 0 & -\mathrm{G}_{\mathcal{T}} & -\mathrm{G}_{\mathcal{F}} & 0 & 0 & 0 \\ \mathrm{G}^{\dagger}_{\mathcal{T}} & \Sigma^{\mathrm{F}}_{\mathcal{T}\mathcal{T}} & \Sigma^{\mathrm{F}}_{\mathcal{T}\mathcal{F}} & 0 & 0 & 0 \\ \mathrm{G}^{\mathcal{F}}_{\mathcal{F}} & \Sigma^{\mathrm{F}}_{\mathcal{F}\mathcal{T}} & \Sigma^{\mathrm{F}}_{\mathcal{F}\mathcal{F}} & 0 & 0 & \mathrm{C}_\Gamma \\ 0 & 0 & 0 & 0 & -\mathrm{E}_{\mathcal{T}} & -\mathrm{E}_{\mathcal{F}} \\ 0 & 0 & 0 & \mathrm{E}^{\dagger}_{\mathcal{T}} & \Sigma^{\mathrm{S}}_{\mathcal{T}\mathcal{T}} & \Sigma^{\mathrm{S}}_{\mathcal{T}\mathcal{F}} \\ 0 & 0 & -\mathrm{C}^{\dagger}_\Gamma & \mathrm{E}^{\dagger}_{\mathcal{F}} & \Sigma^{\mathrm{S}}_{\mathcal{F}\mathcal{T}} & \Sigma^{\mathrm{S}}_{\mathcal{F}\mathcal{F}} \end{bmatrix} \begin{bmatrix} \mathrm{V}^{\mathrm{F}}_{\mathcal{T}} \\ \mathrm{P}_{\mathcal{T}} \\ \mathrm{P}_{\mathcal{F}} \\ \mathrm{S}_{\mathcal{T}} \\ \mathrm{V}^{\mathrm{S}}_{\mathcal{T}} \\ \mathrm{V}^{\mathrm{S}}_{\mathcal{F}} \end{bmatrix} = \begin{bmatrix} 0 \\ \mathrm{G}_{\mathcal{T}} \\ 0 \\ 0 \\ \mathrm{F}_{\mathcal{T}} \\ 0 \end{bmatrix}$$

Propagation of an acoustic (water) pulse into an elastic medium (granit)

- **Simulation parameters:**
  - ▸ **Computational domain:**
    - **Water** on the upper side
    - **Granit** on the lower side
  - ▸ **Mixed-order discretization:** $k' = k + 1 = 3$
  - ▸ **Homogeneous Dirichlet conditions**
  - ▸ **Intial condition:** velocity Ricker wave in the acoustic medium:

$$\boldsymbol{v}_{\mathbf{0}}^{\mathrm{F}}(x, y) := \theta \exp\left(-\pi^2 \frac{r^2}{\lambda^2}\right) (x - x_c, y - y_c)^{\mathrm{T}}$$

  - ▸ **Time integration scheme:** SDIRK(3,4)
  - ▸ **Time step:** $\mathrm{dt} = 0,1 \times 2^{-9}$

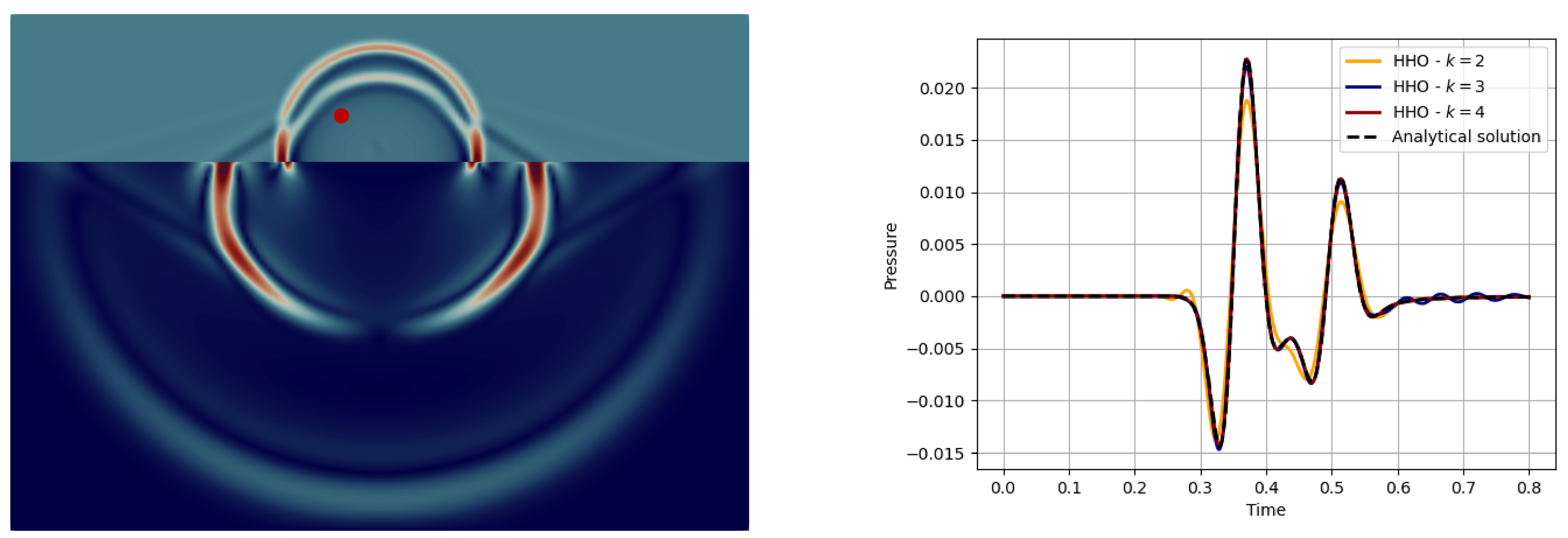

Fig. 5: Left panel: Two-dimensional distribution of the acoustic pressure and the elastic velocity norm, at $t = 0,4375$ s. Right panel: Pressure as a function of time at the sensor in the water (coarse mesh).

General principles of the HHO method

- **HHO is a finite element method similar to Hybrid Discontinuous Galerkin method (HDG)**

Design of the HHO method

- **Degrees of freedom:**
  - ▸ Polynomial unknowns located in the cells (degree k') and on the faces (degree k): $\quad \hat{\boldsymbol{u}}_h := (\boldsymbol{u}_{\mathcal{T}}, \boldsymbol{u}_{\mathcal{F}})$
  - ▸ Equal-order discretization: $k' = k$
  - ▸ Mixed-order discretization: $k' = k + 1$
- **Operators:**
  - ▸ Gradient reconstruction operator: $\boldsymbol{\nabla u} \rightarrow \mathrm{G}(\hat{\boldsymbol{u}}_h)$,
  - ▸ Stabilization operator: $\mathrm{s}(\hat{\boldsymbol{u}}_h, \hat{\boldsymbol{w}}_h)$
    - Penalization at the element level to ensure stability while preserving the approximation properties of the reconstruction.

Advantages over classical finite element methods

- **Mesh flexibility:**
  - ▸ Complex geometries
  - ▸ Unstructured and polyhedral meshes
  - ▸ Local mesh refinement
- **Local conservativity**
- **Optimal error estimates for smooth solutions**
- **Attractive computational costs:**
  - ▸ Global problem couples only face dofs
  - ▸ Cell dofs recovered by local post-processing

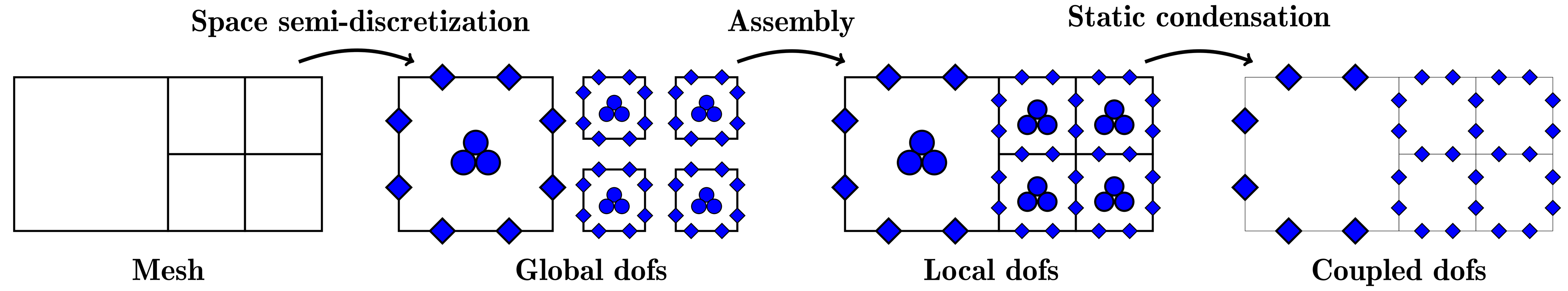

Fig. 2: Static condensation procedure.

Validation on academic test cases

- **Verification of convergence rates on sinusoïdal analytical solutions:**
  - ▸ $\mathcal{O}(h^{k+1})$ in H^1-norm
  - ▸ $\mathcal{O}(h^{k+2})$ in L^2-norm **(superconvergence)**
- **Verification of the energy conservation of the scheme with a no contrast test case:**
  - ▸ $\rho_{\mathrm{S}} = \rho_{\mathrm{F}} = 1, \quad c^{\mathrm{P}}_{\mathrm{S}} = c^{\mathrm{P}}_{\mathrm{F}} = \sqrt{3}, \quad c^{\mathrm{S}}_{\mathrm{S}} = 1$
  - ▸ **Initial condition:** velocity Ricker wave in the acoustic medium:

$$\boldsymbol{v}_{\mathbf{0}}^{\mathbf{F}}(x, y) := \theta \exp\left(-\pi^2 \frac{r^2}{\lambda^2}\right) (x - x_c, y - y_c)^{\mathrm{T}}$$

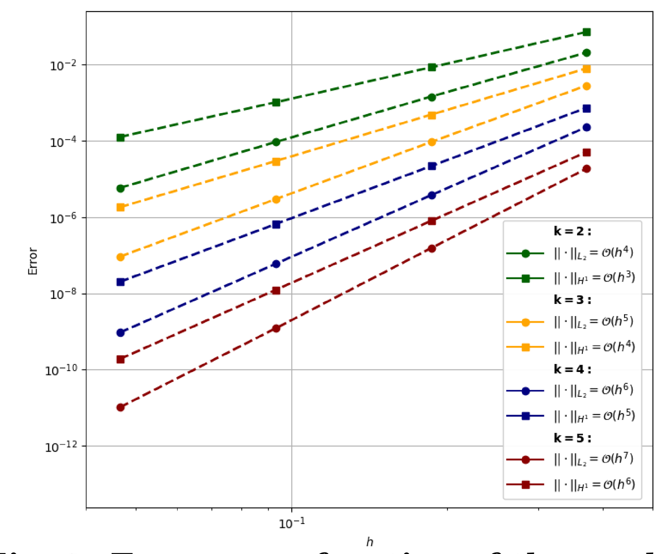

Fig. 3: Errors as a function of the mesh size with $\Delta t = 0.1 \times 2^{-5}$.

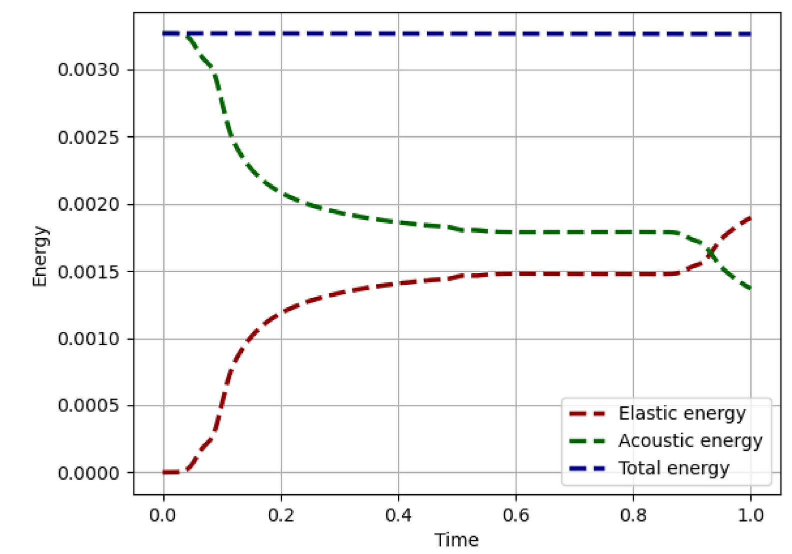

Fig. 4: Repartition of the elastic and acoustic energy after propagation of the wave.

Propagation of an elastic pulse into a sedimentary bassin

- **Composition of the sedimentary bassin:**
  - ▸ **Acoustic region:** air
  - ▸ **Sedimentary region:** $\rho = 1200$ kg.m^3, $c_{\mathrm{P}} = 3400$ m.s^{-1}, $\quad c_{\mathrm{S}} = 1400$ m.s^{-1}
  - ▸ **Elastic region:** $\rho = 5350$ kg.m^3, $c_{\mathrm{P}} = 3090$ m.s^{-1}, $\quad c_{\mathrm{S}} = 2570$ m.s^{-1}

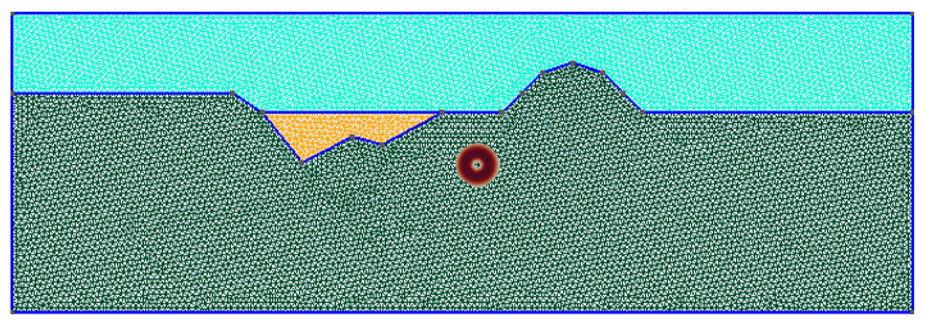

Fig. 6: Mesh of a sedimentary bassin and location of the initial pulse.

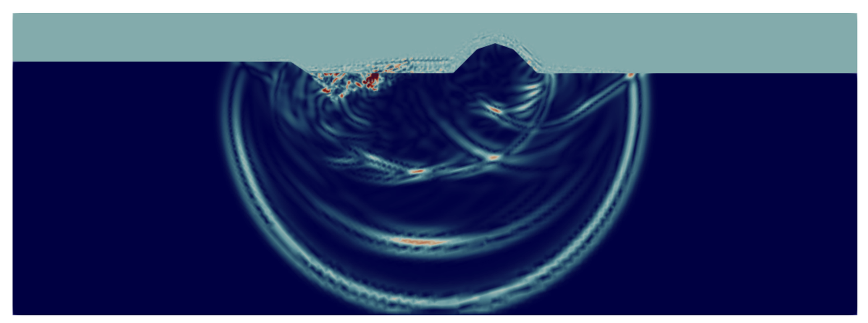

Fig. 7: Progation through the sedimentary bassin.

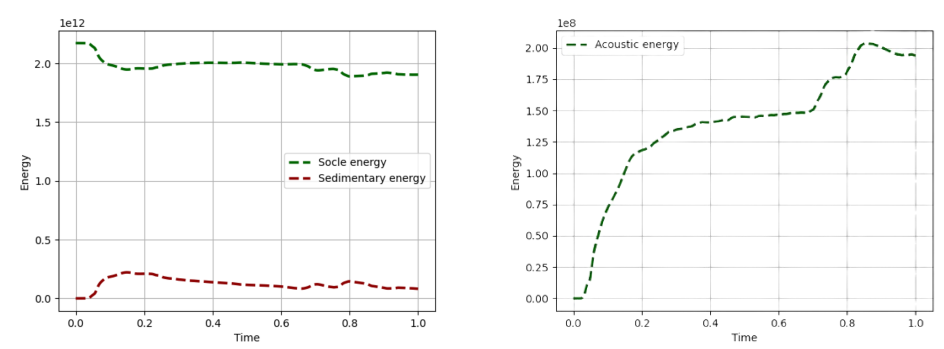

Fig. 8: Repartition of the elastic (left) and the acoustic (right) energy.

Some references

[1] Burman, Duran, and Ern. "Hybrid high-order methods for the acoustic wave equation in the time domain". In: *Comm. App. Math. Comp. Sci.* 4.2 (2022), pp. 597–633.

[2] Di Pietro and Ern. "A hybrid high-order locking-free method for linear elasticity on general meshes". In: *Comput. Meth. Appl. Mech. Engrg.* 283 (2015), pp. 1–21.

[3] Terrana, Vilotte, and Guillot. "A spectral hybridizable discontinuous Galerkin method for elastic-acoustic wave propagation". In: *Geophys. J. Int.* 213.1 (2017), pp. 574–602.